Tree Physiology 35, 1356–1365
doi:10.1093/treephys/tpv074

Research paper

Correlations between morpho-anatomical changes and radial hydraulic conductivity in roots of olive trees under water deficit and rewatering

Giuseppe Tataranni[1,5], Michele Santarcangelo[2], Adriano Sofo[3], Cristos Xiloyannis[1], Stephen D. Tyerman[4] and Bartolomeo Dichio[1]

[1]Dipartimento delle Culture Europee e del Mediterraneo, Università degli Studi della Basilicata, Via San Rocco 3, 75100 Matera, Italy; [2]Dipartimento di Scienze, Università degli Studi della Basilicata, Via dell'Ateneo 10, 85100 Potenza, Italy; [3]Scuola di Scienze Agrarie, Forestali, Alimentari ed Ambientali, Università degli Studi della Basilicata, Via dell'Ateneo 10, 85100 Potenza, Italy; [4]Australian Research Council Centre of Excellence in Plant Energy Biology, Waite Research Institute, School of Agriculture, Food and Wine, University of Adelaide, PMB1, Glen Osmond, SA, 5064, Australia; [5]Corresponding author (giuseppe.tataranni@unibas.it)

Received October 28, 2014; accepted July 15, 2015; published online October 7, 2015; handling Editor Roberto Tognetti

The effects of prolonged drought were studied on olive (*Olea europaea* L.; drought-sensitive cultivar Biancolilla and drought-tolerant cultivar Coratina) to examine how morpho-anatomical modifications in roots impact on root radial hydraulic conductivity (L_{pr}). Two-year-old self-rooted plants were subjected to a gradual water depletion. The levels of drought stress were defined by pre-dawn leaf water potentials (Ψ_w) of −1.5, −3.5 and −6.5 MPa. After reaching the maximum level of drought, plants were rewatered for 23 days. Progressive drought stress, for both cultivars, caused a strong reduction in L_{pr} (from 1.2 to 1.3×10^{-5} m MPa^{-1} s^{-1} in unstressed plants to 0.2–0.6 $\times 10^{-5}$ m MPa^{-1} s^{-1} in plants at $\Psi_w = -6.5$ MPa), particularly evident in the more suberized (brown) roots, accompanied with decreases in stomatal conductance (g_s). No significant differences in L_{pr} and g_s between the two olive cultivars were observed. Epifluorescence microscopy and image analyses revealed a parallel increase of wall suberization that doubled in white stressed roots and tripled in brown ones when compared with unstressed plants. In drought-stressed plants, the number of suberized cellular layers from the endodermis towards the cortex increased from 1–2 to 6–7. Recovery in L_{pr} during rewatering was correlated to the physical disruption of hydrophobic barriers, while the time necessary to obtain new mature roots likely accounted for the observed delay in the complete recovery of g_s. Radial hydraulic conductivity in olive roots was strongly influenced by soil and plant water availability and it was also modulated by structural root modifications, size, growth and anatomy. These findings could be important for maintaining an optimal water status in cultivated olive trees by scheduling efficient irrigation methods, saving irrigation water and obtaining yield of high quality.

Keywords: apoplastic barriers, drought stress, microscopic analyses, stomatal conductance, suberin lamellae, water relations.

Introduction

Root hydraulic conductivity decreases in plants subjected to drought stress (Nobel and Lee 1991, Cruz et al. 1992, Nobel 1992, Lo Gullo et al. 1998, North and Nobel 1998, Huang and Gao 2000, Steudle 2000, Hose et al. 2001) and other stresses, such as salinity, nutrient deficiency, anoxia, temperature and heavy metals (Enstone and Peterson 2005). Though all these stresses have been reported to reduce total root hydraulic conductivity, it is still not clear to what extent the different pathways and resistances of radial flow across the root influence the reduction in root radial hydraulic conductivity (L_{pr}).

Root radial hydraulic conductivity, measured under various conditions, varies with the flow rate and according to the way in which the radial water potential gradient is established. In fact,

roots behave not as a simple membrane, but as complex barriers with radial flow occurring via parallel pathways, comprising the trans-cellular and apoplastic pathways. Each is characterized by a different resistance to water flow and a different response to osmotic gradients (Steudle 2000), but probably not pressure gradients (Chaumont and Tyerman 2014). Depending on the developmental state of the apoplastic barriers, the overall resistance can be distributed across the root cylinder (e.g., in young unstressed roots) or concentrated in certain layers (e.g., exodermis and endodermis in older stressed roots) (Bramley et al. 2009). The radial water flow is also influenced by the frequency of the plasmodesmata, aquaporins (Tyerman et al. 1999, Willigen et al. 2004, Velikanov and Belova 2005, Ye and Steudle 2006) and hydrophilic micropores that can traverse the suberin lamellae (Robards et al. 1979, Peterson 1988).

Studies on different plant species, such as sorghum (Cruz et al. 1992), maize (Frensch and Steudle 1989), wheat (Jones et al. 1988), barley (Sanderson 1983), agave (Nobel and Sanderson 1984, North and Nobel 1998), onion (Melchior and Steudle 1993) and opuntia (Dubrovsky et al. 1998) have shown that L_{pr} varies along the length of the root in relation to the maturation phase. Variations in L_{pr} have also been associated closely with suberization of endodermis and exodermis (Degenhardt and Gimmler 2000, Steudle 2000, Hose et al. 2001, Enstone and Peterson 2005) and the presence of lateral roots (Sanderson 1983, Cruz et al. 1992, Lo Gullo et al. 1998, North and Nobel 1998). The endodermis is constituted of one layer of cells, lacking intercellular spaces, with narrow thickenings (the bands of Caspary) in the radial and cross-sectional walls. In correspondence to these thickenings, the plasma membrane closely joins to the cellular wall that is lignified or suberized, therefore making the wall more hydrophobic (Schreiber et al. 1999). The exodermis has a structure similar to the endodermis and is present in the mature regions of primary roots of many angiosperm species (Hose et al. 2001, Enstone and Peterson 2005), where it acts as a supplementary, selective initial barrier to radial water movement (Steudle and Frensch 1996, Steudle and Peterson 1998, Steudle 2000, 2001).

Olive (*Olea europaea* L.) is often exposed to prolonged dry periods during which high light and high temperatures occur together. Compared with other fruit tree species, this species is able to tolerate low availability of soil water by means of morphological and physiological adaptations acquired in response to perennial drought stress conditions (Gucci et al. 2002, Torres-Ruiz et al. 2011, Rossi et al. 2013). In olive, a series of strategies act together in response to drought stress, including a tight regulation of stomata and transpiration (Rossi et al. 2013), reduction of gas exchange (Moriana et al. 2002), a highly developed osmotic adjustment (Dichio et al. 2006), the up-regulation of some antioxidant enzymes (Sofo et al. 2005), the appearance of anatomical alterations (Bosabalidis and Kofidis 2002), the ability to extract water from deep soil layers, and a large water potential gradient between canopy and roots (Xiloyannis et al. 1999). It has been demonstrated that, during the first days of water recovery following drought release in olive trees, leaf water potential, gas exchange, chlorophyll fluorescence indices (Angelopoulos et al. 1996, Sofo et al. 2005, 2009) and osmotic potential (Dichio et al. 2006) are just partially restored. Particularly, alag in the recovery of full stomatal conductance (g_s), referred to here as stomata inertia, observed during the recovery phase in olive tree could be also linked to root structural changes that reduce the efficiency of axial (e.g., by embolism and/or cavitation) and radial water transport (e.g., by the increase of suberification). Furthermore, the capacity of root systems to recover L_{pr} following drought stress is a crucial aspect of plant adaptation to seasonal drought, especially in the case of sclerophyllous Mediterranean tree species (Salleo 1983, Lo Gullo et al. 1998).

On this basis, the present work investigates the effects of an imposed drought on root radial hydraulic conductivity and root anatomy–morphology in two cultivars of olive that differ in drought tolerance. It is hypothesized that root radial hydraulic conductivity during drought and the following recovery is dependent on the formation and disruption, respectively, of apoplastic barriers and/or on other morphological adjustments occurring in roots.

Materials and methods

Plant material and experimental design

Trials were carried out on 2-year-old self-rooted olive plants (*O. europaea* L.; cv. 'Coratina' and 'Biancolilla'), measuring 1.3–1.5 m in height and having a similar vegetative behaviour. The cultivar Coratina is characterized by high-yield crop and tolerance of water deficit, while Biancolilla is particularly sensitive to drought stress and presents leaves reduced in size (Sofo et al. 2009). The study site was located at the 'Pantanello Agricultural Experimental Station' in Metaponto (Southern Italy; N 40°24′, E 16°48′). The experimental period started on 12 July 2005 and ended on 26 August 2005.

Olive plants grew uniformly outdoors, transplanted in 0.016 m^3 pots, filled with a mixture of sand (73.2%), silt (13.3%) and clay (13.5%). Plants were fertilized, at 25-day intervals throughout the period of vegetative growth, with 3.5 g per pot of slow-release nitrogen complex fertilizer (Nitrophoska Gold 15N-9P-16K + 2Ca + 7Mg; Compo Agricoltura, Cesano Maderno, Italy). Pots were covered with plastic film and aluminium foil in order to avoid evaporation from the soil surface and to minimize temperature increase inside the containers. Soil water content was maintained at ~85% of water holding capacity by integrating the transpiration losses during the day (optimal water status), measured by weighing the pot.

Starting from 13 July, 26 plants per group were subjected to gradual water depletion for 21 days. During the first 10 days of the drought period, plants received in the evening (20 : 00 h)

80% of their water consumption, in order to allow the induction and expression of adaptation mechanisms against drought. Successively, after 11 days of drought application, plants were not irrigated at all. The levels of drought stress in plants were defined by means of the values of leaf water potentials measured pre-dawn (Ψ_w): −1.5 MPa (7–10 days from the beginning of the stress period); −3.5 MPa (14–17 days); −6.5 MPa (20–21 days). After reaching the maximum level of drought (3 August), plants were rewatered. The rewatering lasted 23 days, and during this period the amount of water added daily was equal to the transpired amount. Measurements during the rewatering were carried out after 7 and 23 days from the beginning of water recovery.

Environmental and physiological parameters

Environmental parameters for each day of the experimental period were monitored by a weather station placed within 200 m of the experimental plot. Leaf-to-air vapor pressure deficit (VPD) was calculated according to Goudrian and Van Laar (1994). The values of photosynthetically active radiation (PAR) were recorded at 1-min intervals and daily-integrated (LI-6400; LI-COR Inc., Lincoln, NE, USA). The values of Ψ_w were measured at 04:00–05:00 h at 2–3 day intervals on fully expanded leaves selected along the median segment of new-growth shoots, by using a Scholander pressure chamber (PMS Instrument Co., Albany, OR, USA).

Stomatal conductance was measured using a programmable, open-flow portable system (LI-6400; LI-COR Inc.) operated at 500 μmol s^{-1} flow rate and with a leaf chamber fluorometer (LI-6400-40; LI-COR Inc.). The measurements were carried out at 09:00–10:00 h on fully expanded, horizontally positioned leaves taken from three plants having the same Ψ_w. The temperature inside the leaf chamber was maintained equal to the environmental air temperature by instrument automatic temperature regulation.

Root sampling

Three plants per each drought stress and rewatering level were randomly selected and destructively sampled once they reached each determined value of Ψ_w. Plant roots were washed accurately, using weak water flow to avoid damage, and root samples were taken as six apical branched portions from every plant. Structural and old roots (over 2 mm in diameter) were not chosen. Uniform young roots of known age, as they developed after transplanting in the space occupied by new soil, were considered representative of the experimental conditions. These samples were divided into two groups, according to their morphology and color (white and brown roots), and used to measure L_{pr} and carry out microscopic analyses.

Root hydraulic conductivity

Each root sample was positioned inside the chamber after having cut the terminal portion in water and connected via a silicone tube to a needle in the chamber cap. The excised root system was immersed in a beaker containing pre-aerated pure water. The chamber was pressurized using nitrogen. Root exudate was collected in a sealed Eppendorf tube to avoid evaporation and weighed at 10 and 20 min after pressurization. Total root surface area of the samples was calculated by $2\pi r \times$ root length.

Root radial hydraulic conductivity, that is the volume of water crossing the root surface per unit area per unit time and per unit driving force ($m^3\ m^{-2}\ MPa^{-1}\ s^{-1}$, equivalently, $m\ MPa^{-1}\ s^{-1}$) was measured as $L_{pr} = L_{root}/A_s$, where L_{root} is the root radial hydraulic conductance and A_s is the conducting surface area. Root radial hydraulic conductance ($m^3\ Pa^{-1}\ s^{-1}$) was measured as $L_{root} = J_v/\Delta\Psi_w$; where J_v is the rate of water flow ($m^3\ s^{-1}$) and $\Delta\Psi_w$ is the radial water potential difference across the root. A pressure chamber technique was used to measure J_v as a function of $\Delta\Psi_w$ (Lang and Ryan 1994, Dichio et al. 2003).

Image analysis

Root samples were stored in formaldehyde after L_{pr} measurement. Root apical portions per each drought stress and rewatering level were subsequently fixed in alcohol and embedded in JB-4 resin (JB-4 Embedding Kit®, Tebu-Bio S.r.l., Milan, Italy). Three root cross-sections (≤1 mm in diameter and ~15 μm thick) per each drought stress and rewatering level were obtained using a rotating microtome at ~6 mm from the root tip and observed with an optical microscope (Axiophot, ZEISS, Oberkochen, Germany) under transmission light and a mercuric vapor lamp HBO 50 at 100 and 200× magnifications to check epifluorescence emissions. For the epifluorescence quantification, the 2D-images were digitalized and converted in grey scale (RGB). On the basis of RGB light level variation, the same images were represented as 3D images (Surface Plot). After subtracting a background level outside of the exodermis and endodermis, it was possible to measure the integrals of the studied area overcoming the so defined RGB threshold light level.

The three best photographs (by a 35 mm film) were taken from every section in order to evaluate the following root morpho-anatomical parameters: cell wall suberization degree (by epifluorescence quantification), root section circularity index, intercellular spaces area, cell number per unit area and cell size (in terms of cross-sectional area). The software ImageJ 1.37v (W. Rasband, National Institutes of Health, Bethesda, MD, USA) was used to measure root morpho-anatomical parameters, and at least five measurements per image were carried out. Regarding root section circularity, an arbitrary and a dimensional index (range = 0–1, where 1 = perfect circle) was automatically assigned to every root section by the software to evaluate the approximation of the root section itself to a perfect circle.

Statistical analysis

The values of Ψ_w represent the mean of measurements (±SE) on three leaves on each of three selected plants, whereas the

values of g_s represent the mean of measurements (±SE) on three leaves per plant on each of three selected plants for each drought and rewatering level. The values of L_{pr} were taken from three root models of three plants for each drought and rewatering level. Regarding image analysis, three photographs for each of three root cross-sections per plant at each drought and rewatering level were considered.

To determine whether the above analyzed parameters and L_{pr} were related, correlation analysis was performed (Pearson's correlation coefficient; R). Linear and non-linear regression analyses were performed to examine the relationship between root morphology and root water transport, selecting the best fits that minimized the absolute sum of squares (R^2 and significance). The statistical analysis of data was carried out using the Sigmastat 3.1 SPSS Inc. software (SPSS Inc., Chicago, IL, USA). Analysis of variance (ANOVA) of all the studied parameters was performed with drought stress levels as factors. Means were statistically analyzed by Fisher's LSD test at $P \leq 0.05$ and $P \leq 0.01$.

Results

Environmental conditions

During the experimental period, the levels of daily PAR exhibited a constant trend with high values under clear sky between 1700 and 1900 μmol m^{-2} s^{-1} at 12:00 h, between 50 and 70 mol m^{-2} day^{-1}, except for some cloudy days. Maximum VPD ranged from 2.0 (on 11 August) to 5.4 kPa (on 29 July) and during the rewatering it was, on average 2.9 kPa. Maximum air temperatures ranged between 34.2 °C (3 August) and 29.0 °C (13 July), with a mean value of 31.6 °C during the whole experimental period.

Water potential and gas exchange

In all plants under drought, Ψ_w of selected plants gradually decreased reaching a mean value of −6.5 MPa after 21 days, and successively recovered completely during rewatering. Stomatal conductance decreased with increasing drought in both the cultivars (Table 1). At the end of the recovery period, the values of g_s (0.16 and 0.11 mol m^{-2} s^{-1} for Coratina and Biancolilla, respectively) did not recover to the values of unstressed plants at the beginning of the experiment (0.22 and 0.15 mol m^{-2} s^{-1} for Coratina and Biancolilla, respectively) (Table 1).

Root hydraulic conductivity

The progressing drought stress, for both the olive tree cultivars, Biancolilla and Coratina, caused a strong reduction in root radial hydraulic conductivity, L_{pr}, from the mean value of unstressed plants of ~1.2×10^{-5} to 0.3×10^{-5} m MPa^{-1} s^{-1} (Figure 1). The greatest variation occurred, however, after 20 days of drought stress and particularly in brown roots (more suberized roots) (Figure 1). A gradual resumption of L_{pr} to the levels of unstressed plants at the beginning of the experiment was observed in the phase of water recovery, and it was quicker in white roots (after ~10 days) than in brown ones (comparable values after 25 days) (Figure 1).

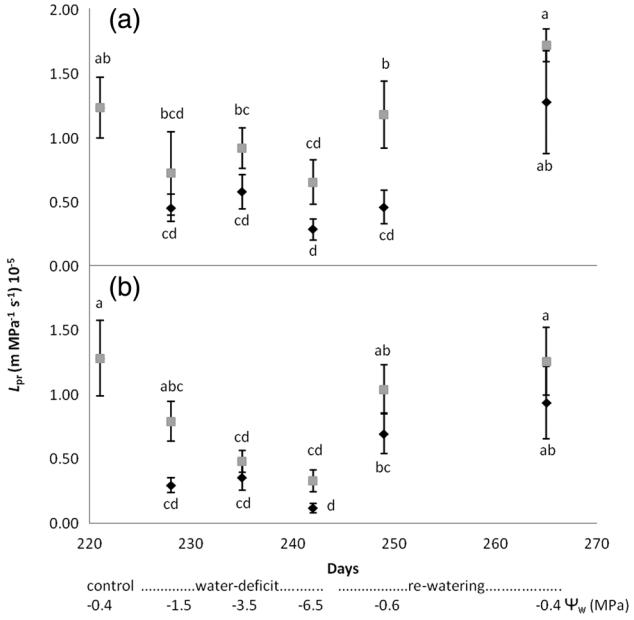

Figure 1. Root hydraulic conductivity (L_{pr}) in white (grey squares) and brown (black diamonds) roots of Biancolilla (a) and Coratina (b) olive cultivars under drought and rewatering. Letters indicate significant differences between days ($P \leq 0.05$, according to Fisher's LSD test).

Table 1. Pre-dawn leaf water potential (Ψ_w) and stomatal conductance (g_s) in Biancolilla and Coratina olive plants before drought stress (unstressed), at different drought stress levels ($\Psi_w = -1.5$, −3.5 and −6.5 MPa) and following recovery (first and second level). Values (mean ± SE) followed by different letters are significantly different between columns ($P \leq 0.05$, according to Fisher's LSD test).

	Unstressed	Drought stressed			Rewatered	
		−1.5 MPa	−3.5 MPa	−6.5 MPa	First level	Second level
Coratina						
Ψ_w (MPa)	−0.40 ± 0.04^a	−1.51 ± 0.11^b	−3.46 ± 0.07^c	−6.45 ± 0.10^d	−0.56 ± 0.10^a	−0.40 ± 0.03^a
g_s (mol m^{-2} s^{-1})	0.22 ± 0.03^a	0.06 ± 0.01^c	0.04 ± 0.01^d	0.03 ± 0.01^d	0.15 ± 0.02^b	0.16 ± 0.03^b
Biancolilla						
Ψ_w (MPa)	−0.40 ± 0.02^a	−1.54 ± 0.11^b	−3.49 ± 0.12^c	−6.52 ± 0.09^d	−0.60 ± 0.03^a	−0.40 ± 0.03^a
g_s (mol m^{-2} s^{-1})	0.15 ± 0.02^a	0.04 ± 0.01^c	0.04 ± 0.01^c	0.03 ± 0.01^d	0.05 ± 0.01^c	0.11 ± 0.02^b

The analysis of the variance of L_{pr} did not show significant differences between the two genotypes, but white roots always had a higher conductivity. There was no interaction between 'cultivar' and 'color'. The two-way ANOVA for L_{pr} evidenced that there were no differences between the two genotypes, but that L_{pr} was strongly influenced by water availability. Modifications occurring at root level seem to influence directly L_{pr} and its trend (Table 2; see Figure 5a).

Microscopy and image analysis

The image analysis of root cross sections (surface plotting based on RGB histograms and following measurements of interesting area integrals overcoming a defined light threshold) allowed quantification of the increase of cell wall suberization processes at the exodermis and endodermis (Figures 2–4). Suberization was expressed in an average percentage (on total cross section) of the epifluorescent area (integral of the area overcoming a defined RGB threshold level) (Figure 4). At $\Psi_w = -3.5$ MPa, suberization doubled in stressed white roots and tripled in brown ones, compared with unstressed plants. The brown roots reached higher levels of suberization in all the three levels of stress (on average from 15% of total cells in unstressed plants to 50% in plants at $\Psi_w = -3.5$ MPa). At the maximum level of drought, cell walls were damaged (Figures 2 and 3) and the measured epifluorescence was lower than in the previous stress levels (Figure 4). The differences in suberization were statistically different among roots of unstressed, drought-stressed and recovered plants, while those between cultivars at the same drought level were not significant (Figure 4). Interestingly, the quantified level of suberization (x; Figure 4) was linearly and inversely related to L_{pr} (y), Coratina: $y = -43.19x + 1.34$, $R^2 = 0.62$, $P = 0.01 < 0.05$; Biancolilla: $y = -53.14x + 1.60$, $R^2 = 0.70$, $P = 0.01 < 0.05$ (Table 2; Figure 5a). In drought-stressed plants of both the cultivars, the number of suberized cellular layers from the endodermis towards the cortex increased from 1–2 to 6–7 (Figure 2).

The mean circularity index of the analyzed sections in both varieties (Figure 6a) varied from 0.9 in roots of unstressed plants, to 0.7–0.6 in drought-stressed roots at $\Psi_w = -6.5$ MPa, finally returning to higher values (0.7–0.8) in rewatered ones. In both the cultivars, observations indicated an increase in intercellular spaces and of the number of dead cortical cells with increasing drought. The mean number of cells per area unit dropped from ~1000 mm^{-2} in unstressed plants to 100 mm^{-2} in plants at $\Psi_w = -6.5$ MPa, and came back to 600 mm^{-2} after the rewatering (Figure 6b). The cells of the endodermis and exodermis layers maintained a constant size throughout the experiment (Figure 2). Root cortical cells, with thin walls, became progressively larger at stress level (from 800 μm^2 in unstressed plants to 4000 μm^2 in plants at $\Psi_w = -1.5$ MPa), and then successively died or reduced their size when drought was prolonged (3000 and 2000 μm^2 at $\Psi_w = -3.5$ and -6.5 MPa, respectively) (Figure 6c). The cortical cells of roots at the two recovery levels ($\Psi_w = -0.6$ and -0.4 MPa), in active division, were smaller and more homogeneous (~1000 μm^2 in size), with a size statistically similar to that of cortical cells in unstressed plants (Figures 2 and 6c).

Discussion

Roots of plants under water deficit can adopt various strategies to survive by a range of morphological, anatomical and physiological adaptations, including deposition/demolition of structural barriers, and expression and modulation of aquaporins (Perez-Martin et al. 2014). In both the olive tree cultivars studied here, drought stress caused a strong reduction in L_{pr} with increasing drought (up to about −75% at $\Psi_w = -6.5$ MPa), particularly in brown and more suberized roots (Figures 1 and 4). Although the methods and samples used were different, these drastic changes in radial conductivity are similar to the declines of root hydraulic conductance observed by Lo Gullo et al. (1998) and Torres-Ruiz et al. (2015) in olive plants subjected to increasing soil dryness. For the two varieties examined here, the trends in hydraulic conductivity were not dependent on olive variety. Indeed, there were no significant differences considering the interactions 'cultivar-drought stress level' or 'cultivar-root color', even though white roots always presented a higher value of L_{pr} (Figure 1).

Root radial hydraulic conductivity varies in relation to the apoplastic barriers that the flow meets, and that apoplastic path can be

Table 2. Correlation matrix with Pearson's correlation coefficients (R) calculated between leaf water potential, root radial hydraulic conductivity and root morpho-anatomical parameters. The values followed by an asterisk are significantly different according to Fisher's LSD test (*$P \le 0.05$; **$P \le 0.01$).

	Pre-dawn leaf water potential (MPa)	Root radial conductivity (m MPa^{-1} s^{-1})	Epifluorescence (%)	Circularity index	Cell density (number mm^{-2})	Cell cross-sectional area (μm^2)
Pre-dawn leaf water potential (MPa)	1.00					
Root radial conductivity (m MPa^{-1} s^{-1})	0.73*	1.00				
Suberization (%)	−0.67*	−0.81*	1.00			
Circularity index	0.75*	0.90*	−0.69*	1.00		
Cell density (number mm^{-2})	0.76*	0.84*	−0.78*	0.88**	1.00	
Cell cross-sectional area (μm^2)	−0.40*	−0.81*	0.71*	−0.77*	−0.79*	1.00

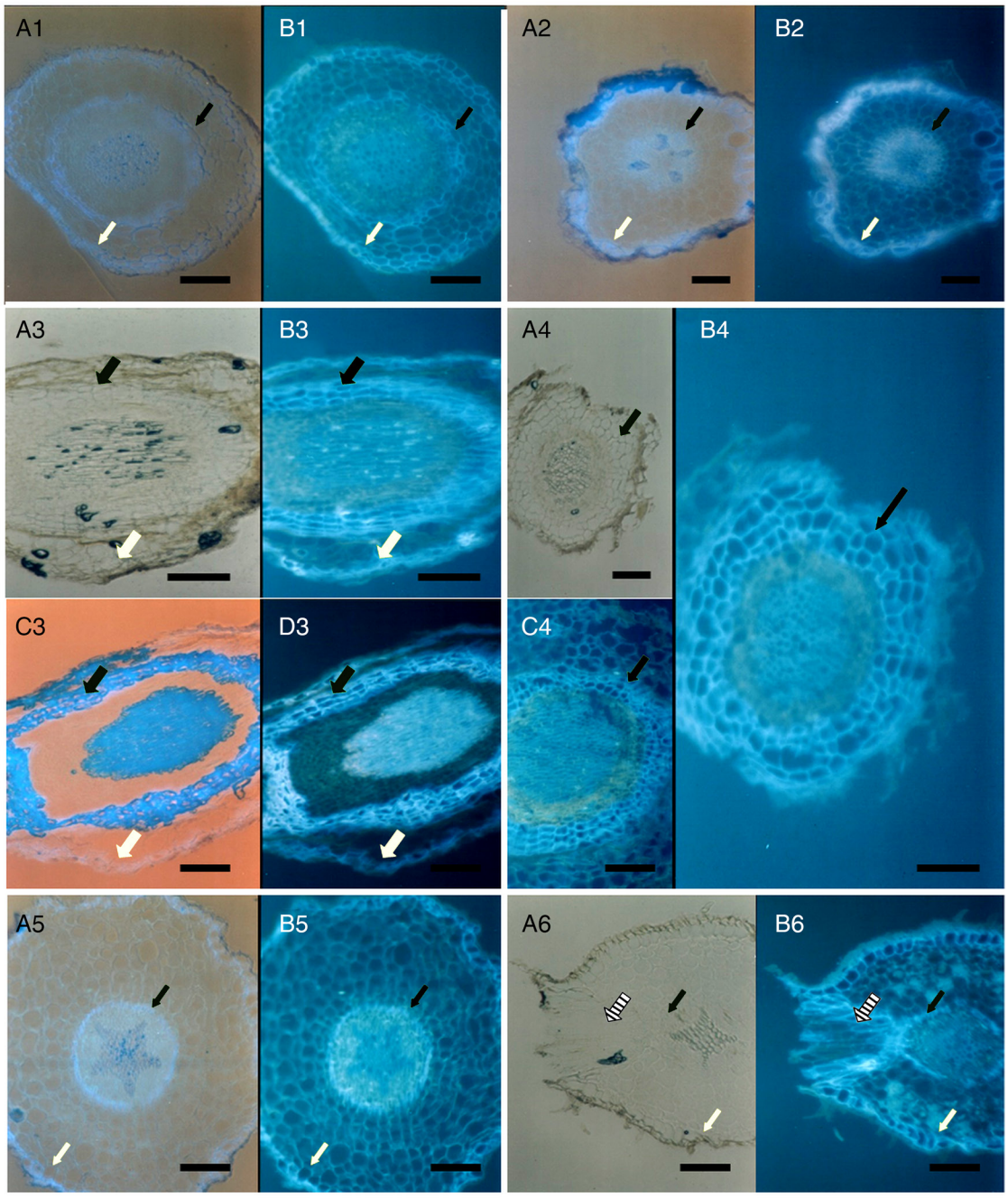

Figure 2. Cross sections of olive roots (≤1 mm) observed and photographed using an optical microscope. (1) Unstressed; (2) first level of stress, $\Psi_w = -1.5$ MPa; (3) second level of stress, $\Psi_w = -3.5$ MPa; (4) third level of stress, $\Psi_w = -6.5$ MPa; (5) first level of recovery; (6) second level of recovery. a1, a2, c3 and a5 were obtained exposing the preparations to transmitted light and overlapping the mercuric lamp for epifluorescence; a3, a4, a6 to transmitted light; b1, b2, b3, d3, b4, c4, b5 and b6 to mercuric lamp. The white arrows indicate the exodermis, the black arrows the endodermis, the striped arrows root primordia. Scale bar (black) = 200 μm.

modified by apoplastic barriers (Casparian strips in the exo- and endodermis, suberin lamellae; Hose et al. 2001, Enstone et al. 2003). Suberin accumulation requires time in the order of hours to days, and requires the activation of specific genes, protein synthesis and polymerization and deposition in the wall (Cottle and Kolattukudy 1982, Lo Gullo et al. 1998). The trends of L_{pr}, especially at high levels of drought stress, were influenced by modifications occurring at the root level (Table 2; Figure 5). Indeed, image analysis data allowed us to define a series of morpho-anatomical responses occurring when roots were subjected to prolonged water deficit (Table 2; Figures 4 and 6). Hydrophobic barriers appeared to be coupled to the measured decreases in L_{pr}, as demonstrated by the negative correlations between the increasing levels of auto-fluorescence (epifluorescence) due to suberin

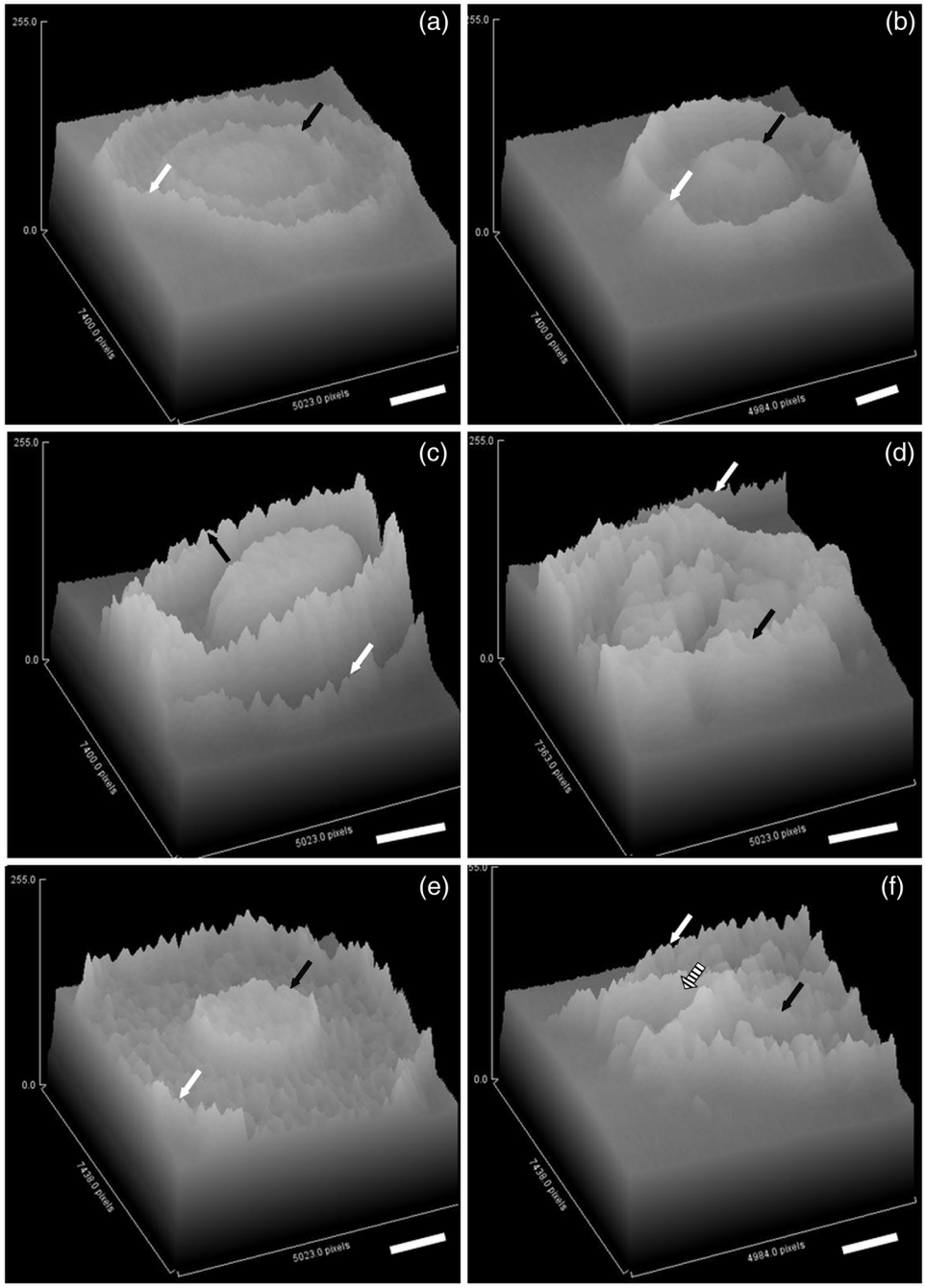

Figure 3. Surface plot of the photographed images: suberization (epifluorescence). (a) Unstressed; (b) first level of stress, $\Psi_w = -1.5$ MPa; (c) second level of stress, $\Psi_w = -3.5$ MPa; (d) third level of stress, $\Psi_w = -6.5$ MPa; (e) first level of recovery; (f) second level of recovery. *x* and *y* axes are in pixels; axis *z*: grey scale (0–255). The white arrows indicate the exodermis, the black arrows the endodermis, the striped arrows root primordia. Scale bar (black) = 200 μm.

accumulation and L_{pr} values (Figures 2–5; Table 2). Particularly, suberin accumulated in the cell walls of the endodermis and exodermis (Figures 2 and 3), in accordance with other authors (Nobel and Sanderson 1984, Cruz et al. 1992, Lo Gullo et al. 1998, Steudle 2000, Hose et al. 2001, Enstone and Peterson 2005). Under drought conditions, the number of suberized layers also increased (Figures 2 and 3). Moreover, suberin accumulation appeared to be an irreversible process, as during rewatering it did not recover to the values of unstressed plants before the drought stress application (Figures 2–4). The suberization dynamics observed here could have a particular importance because, as at high levels of drought, suberin barriers also reduce the water losses due to the passive, free movement of water from the root to the soil through the suberized structures, according to the water potential gradient, so preserving root meristematic vitality and the emergence of lateral roots.

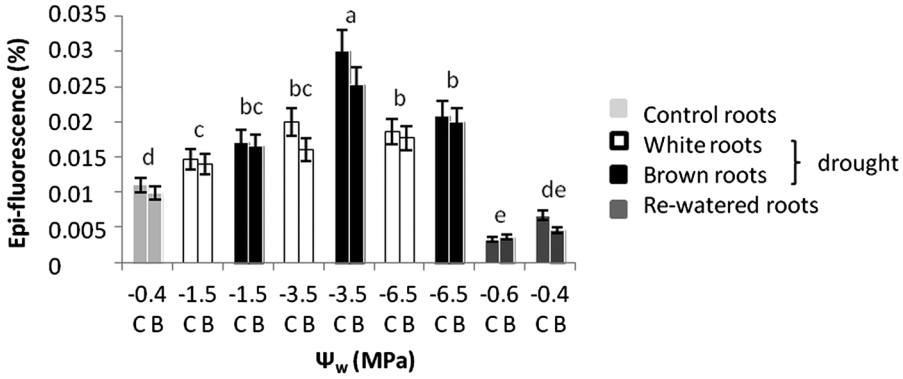

Figure 4. Quantification of the emitted epifluorescence expressed in % (±SE) of the section area for Biancolilla (B) and Coratina (C) olive plants before drought stress (unstressed), at different drought stress levels ($\Psi_w = -1.5$, -3.5 and -6.5 MPa), and following recovery (first and second level). Letters indicate significant differences between drought stress levels. Differences are not significant between cultivars for the same drought stress level ($P \leq 0.05$, according to Fisher's LSD test).

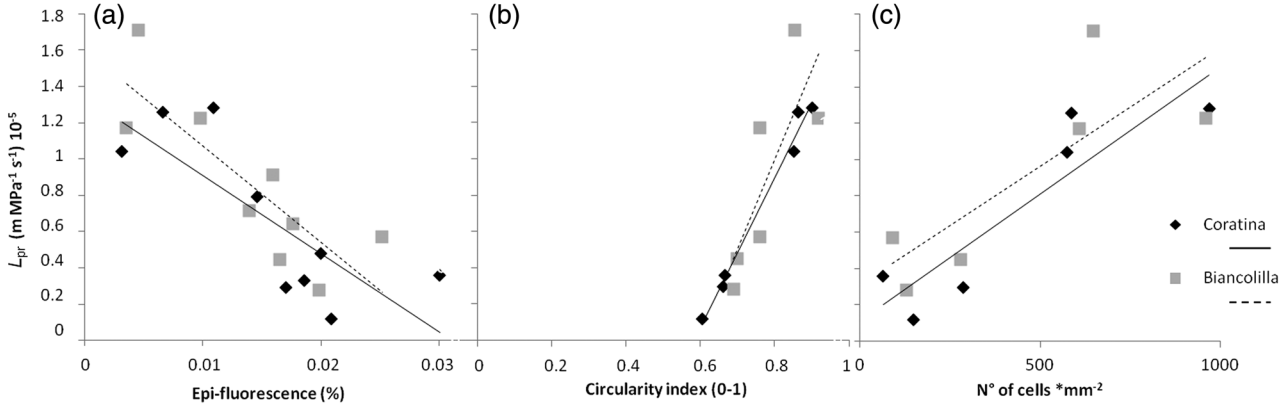

Figure 5. Regression analysis. (a) Hydraulic conductivity (L_{pr}) versus suberization. Coratina: $y = -43.19x + 1.34$; $R^2 = 0.62$; $P = 0.01 \leq 0.05$. Biancolilla: $y = -53.14x + 1.60$; $R^2 = 0.70$; $P = 0.01 \leq 0.05$. (b) Root radial hydraulic conductivity (L_{pr}) versus section circularity index. Coratina: $y = 4.1x - 2.39$; $R^2 = 0.99$; $P = 0.00006 \leq 0.05$. Biancolilla: $y = 4.97x - 2.98$; $R^2 = 0.65$; $P = 0.05 \leq 0.05$. (c) Hydraulic conductivity (L_{pr}) versus mean number of cells per unit area. Coratina: $y = 0.001x + 0.11$; $R^2 = 0.81$; $P = 0.02 \leq 0.05$. Biancolilla: $y = 0.001x + 0.31$; $R^2 = 0.65$; $P = 0.05 \leq 0.05$. The analysis was performed between the mean values of L_{pr} and epifluorescence (suberization) (a), circularity index (b) and number of cells per unit area (c) in Biancolilla and Coratina olive plants before drought stress (unstressed), at different drought stress levels ($\Psi_w = -1.5$, -3.5 and -6.5 MPa), and following recovery (first and second level). Differences are not significant between cultivars ($P \leq 0.05$, according to Fisher's LSD test).

Further morpho-anatomical modifications were correlated with the progressive drought stress and were also linked to the reduction in L_{pr} (Table 2). The circularity index, evaluating the approximation of the root section to a perfect circle in a normal condition of water availability, describes the status of dehydration-damage of roots under drought stress (1 corresponds to circular, unstressed roots, and lower values to more deformed, dry roots), excluding fixation and sectioning interference due to the technology used. Interestingly, root circularity was reduced during drought (Figures 5b and 6a) because shrinkages and deformations due to dehydration and solute concentration likely occurred (Dichio et al. 2003, 2006) when deformations occurred (Figure 2). During the drought phase, the mean number of intact cortical cells decreased (Figures 5c and 6b), probably as a consequence of the inhibition and ultimately block of the mitotic processes (Passioura 2002). The observed increase in intercellular spaces in the cortical zone (Figure 2) was probably caused by shrinkages and cellular death (Figures 2 and 6b). The mean cellular area increased just at the first level of stress ($\Psi_w = -1.5$ MPa), likely as a result of the maintenance of water in the roots due to the synthesis of new solutes (Xiloyannis et al. 1999, Dichio et al. 2003, 2006), but then decreased at more severe drought levels ($\Psi_w = -3.5$ and -6.5 MPa). On the other hand, the mean number of cells per unit area (mm^2) in roots of recovered plants, after drought application, came back to the levels found in well watered ones. The constant size maintained by the cells of the endodermis and exodermis layers during the drought progression was probably due to their rigid wall thickenings, whereas the increased size of cross-sectional area of cortical cells at the beginning of the stress likely allowed them to store water by active and passive osmotic regulation mechanisms.

During recovery, L_{pr} and the root structures gradually returned to the values of unstressed plants (Table 1; Figures 1–3). Lo Gullo et al. (1998) found that when olive plants are rewatered

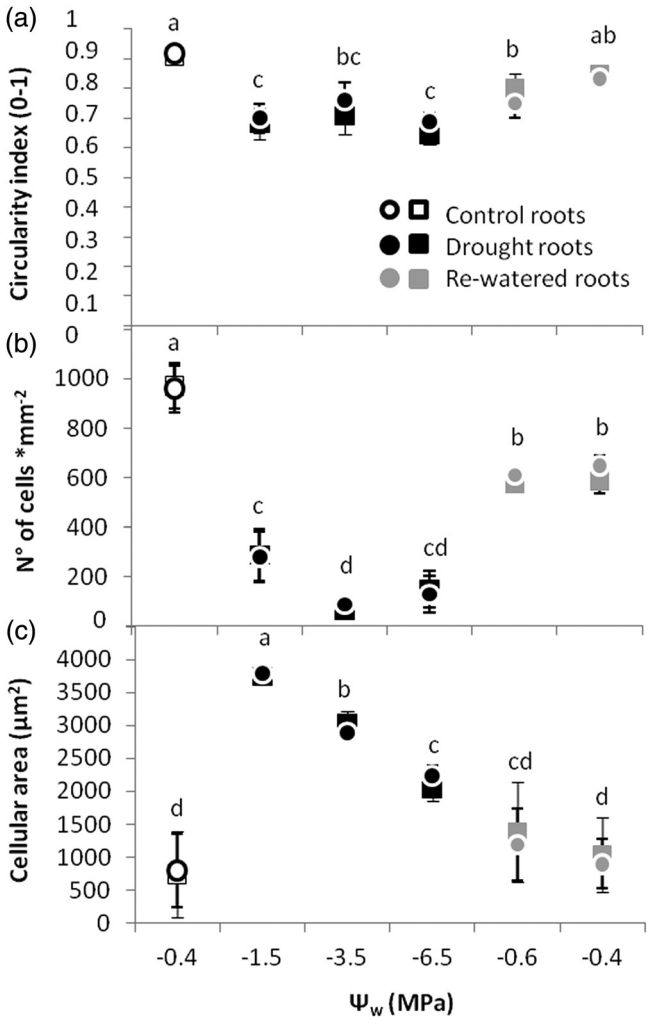

Figure 6. (a) Mean circularity index (arbitrary scale 0–1; ±SE), (b) number of cortex cells per unit root cross section area (±SE) and (c) mean area of cortical cells (µm^2; ±SE) of the root sections analyzed for Biancolilla (round dots) and Coratina (square dots) olive plants before drought stress (unstressed), at different drought stress levels (Ψ_w = −1.5, −3.5 and −6.5 MPa) and following recovery (first and second level). Letters indicate significant differences between drought stress levels; differences are not significant between cultivars for the same drought stress levels ($P \leq 0.05$, according to Fisher's LSD test).

after reaching Ψ_w = 1–2 MPa, the value of root hydraulic conductance increased from 16 to 66% of that measured in unstressed seedlings, but 96 h after rewetting the soil to field capacity did not return to that of unstressed plants. The plant is not able to directly and immediately use or modify complex wall placed molecules (such as suberin). Most plant species synthesize ester-linked aromatics, also called 'aromatic suberin', like *p*-coumaric and ferulic acids, which render cell walls recalcitrant to biodegradation (Schreiber et al. 1999). Thus, new primordia (Figures 2–4), that will form the completely active working roots, should physically emerge and break off the preexisting barriers, outside of the pericycle (Peterson and Moon 1993, Lo Gullo et al. 1998, North and Nobel 1998) (Figures 2 and 3). The time necessary to obtain new mature roots probably accounts for the observed delay (Angelopoulos et al. 1996, Fernández et al. 1997, Sofo et al. 2009) before the complete restoration of root radial hydraulic conductivity (Table 1; Figure 1). The lag in L_{pr} recovery could also have affected stomata conductance (Table 1; Figure 1), but non-hydraulic factors (e.g., production of abscisic acid in dry roots and photoinhibition) cannot be ruled out, as pointed out by Torres-Ruiz et al. (2015) and Sofo et al. (2009), respectively.

The results demonstrated that radial hydraulic conductivity in olive roots was strongly influenced by soil and plant water availability. It was demonstrated that, over periods that simulate environmental drought periods, this parameter is modulated by structural root modifications, size, growth and anatomy. It is possible to affirm that the barrier distribution in olive roots represents one of the important factors determining water relations and root transport properties. Furthermore, under prolonged and severe stress conditions, morpho-anatomical modifications of olive roots are inevitable and irreversible. Hydrophobic barriers reduce radial root conductivity, but at the same time also avoid root dehydration, so preserving meristematic and stele vitality. Considering the economic and cultural importance of olive in the Mediterranean basin, these findings could be important for maintaining an optimal water status in cultivated olive plants by scheduling efficient irrigation methods, saving irrigation water and obtaining yield of high quality.

Conflict of interest

None declared.

Funding

This work was supported by the Italian 'Ministero dell'Istruzione, dell'Università e della Ricerca' (MIUR)—PRIN 2009 (Protocollo 20092MES7A), and by the 'Programma di Sviluppo Rurale (PSR) Basilicata FEARS/2007-2013', Misura 124—PIF Eufolia Mediterranea.

References

Angelopoulos K, Dichio B, Xiloyannis C (1996) Inhibition of photosynthesis in olive trees (*Olea europaea* L.) during water stress and rewatering. J Exp Bot 47:1093–1100.

Bosabalidis AM, Kofidis G (2002) Comparative effects of drought stress on leaf anatomy of two olive cultivars. Plant Sci 163:375–379.

Bramley H, Turner NC, Turner DW, Tyerman SD (2009) Roles of morphology, anatomy, and aquaporins in determining contrasting hydraulic behavior of roots. Plant Physiol 150:348–364.

Chaumont F, Tyerman SD (2014) Aquaporins: highly regulated channels controlling plant water relations. Plant Physiol 164:1600–1618.

Cottle W, Kolattukudy PE (1982) Biosynthesis, deposition, and partial characterization of potato suberin phenolics. Plant Physiol 69:393–399.

Cruz RT, Jordan WR, Drew MC (1992) Structural changes and associated reduction of hydraulic conductance in roots of *Sorghum bicolor* L. following exposure to water deficit. Plant Physiol 99:203–212.

Degenhardt B, Gimmler H (2000) Cell wall adaptations to multiple environmental stresses in maize roots. J Exp Bot 51:595–603.
Dichio B, Xiloyannis C, Angelopoulos K, Nuzzo V, Bufo SA, Celano G (2003) Drought-induced variations of water relations parameters in *Olea europaea*. Plant Soil 257:381–389.
Dichio B, Xiloyannis C, Sofo A, Montanaro G (2006) Osmotic regulation in leaves and roots of olive trees during a water deficit and rewatering. Tree Physiol 26:179–185.
Dubrovsky JG, North GB, Nobel PS (1998) Root growth, developmental changes in the apex, and hydraulic conductivity for *Opuntia ficus-indica* during drought. New Phytol 138:75–82.
Enstone DE, Peterson CA (2005) Suberin lamella development in maize seedling roots grown in aerated and stagnant conditions. Plant Cell Environ 28:444–455.
Enstone DE, Peterson CA, Ma F (2003) Root endodermis and exodermis: structure, function, and responses to the environment. J Plant Growth Regul 21:335–351.
Fernández JE, Moreno F, Girón IF, Blázquez OM (1997) Stomatal control of water use in olive tree leaves. Plant Soil 190:179–192.
Frensch J, Steudle E (1989) Axial and radial hydraulic resistance to roots of maize (*Zea mays* L.). Plant Physiol 91:719–726.
Goudrian J, Van Laar HH (eds) (1994) Modeling potential crop growth processes. Kluwer Academic, Dordrecht, pp 29–49.
Gucci R, Grimelli A, Costagli G, Tognetti R, Minnocci A, Vitagliano C (2002) Stomatal characteristics of two olive cultivars "Frantoio" and "Leccino". Acta Hortic 586:541–544.
Hose E, Clarkson DT, Steudle E, Schreiber L, Hartung W (2001) The exodermis: a variable apoplastic barrier. J Exp Bot 52:2245–2264.
Huang B, Gao H (2000) Root physiological characteristics associated with drought resistance in tall fescue cultivars. Crop Sci 40:196–203.
Jones H, Leigh RA, Wyn Jones RG, Tomos AD (1988) The integration of whole-root and cellular hydraulic conductivities in cereal roots. Planta 174:1–7.
Lang A, Ryan KG (1994) Vascular development and sap flow in apple pedicels. Ann Bot 74:381–388.
Lo Gullo MA, Nardini A, Salleo S, Tyree MT (1998) Changes in root hydraulic conductance (KR) of *Olea oleaster* seedlings following drought stress and irrigation. New Phytol 140:25–31.
Melchior W, Steudle E (1993) Water transport in Onion (*Allium cepa* L.) roots (changes of axial and radial hydraulic conductivities during root development). Plant Physiol 101:1305–1315.
Moriana A, Villalobos FJ, Fereres E (2002) Stomatal and photosynthetic responses of olive (*Olea europaea* L.) leaves to water deficits. Plant Cell Environ 25:395–405.
Nobel PS (1992) Root-soil responses to water pulses in dry environments. In: Caldwell MN, Pearcy RW (eds) Exploitation of environmental heterogeneity by plants: ecophysiological processes above and below ground. Academic Press, San Diego, CA, pp 285–304.
Nobel PS, Lee CH (1991) Variations in root water potentials: influence of environmental factors for two succulent species. Ann Bot 67:549–554.
Nobel PS, Sanderson J (1984) Rectifier-like activities of roots of two desert succulents. J Exp Bot 35:727–737.
North GB, Nobel PS (1998) Water uptake and structural plasticity along roots of a desert succulent during prolonged drought. Plant Cell Environ 21:705–713.
Passioura JB (2002) Soil conditions and plant growth. Plant Cell Environ 25:311–318.
Perez-Martin A, Michelazzo C, Torres-Ruiz JM, Flexas J, Fernández JE, Sebastiani L, Diaz-Espejo A (2014) Regulation of photosynthesis and stomatal and mesophyll conductance under water stress and recovery in olive trees: correlation with gene expression of carbonic anhydrase and aquaporins. J Exp Bot 65:3143–3156.
Peterson CA (1988) Exodermal Casparian bands: their significance for ion uptake by roots. Physiol Plant 72:204–208.
Peterson CA, Moon GJ (1993) The effect of lateral root outgrowth on the structure and permeability of the onion root exodermis. Bot Acta 106:411–418.
Robards AW, Clarkson DT, Sanderson J (1979) Structure and permeability of the epidermal/hypodermal layers of the sand sedge (*Carex arenaria*, L.). Protoplasma 101:331–347.
Rossi L, Sebastiani L, Tognetti R, D'Andria R, Morelli G, Cherubini P (2013) Tree-ring wood anatomy and stable isotopes show structural and functional adjustments in olive trees under different water availability. Plant Soil 372:567–579.
Salleo S (1983) Water relations parameters of two Sicilian species of *Senecio* (Groundsel) measured by the pressure bomb technique. New Phytol 95:179–188.
Sanderson J (1983) Water uptake by different regions of the barley root. Pathways of radial flow in relation to development of the endodermis. J Exp Bot 34:240–253.
Schreiber L, Hartmann K, Skrabs M, Zeier J (1999) Apoplastic barriers in roots: chemical composition of endodermal and hypodermal cell walls. J Exp Bot 50:1267–1280.
Sofo A, Dichio B, Xiloyannis C, Masia A (2005) Antioxidant defences in olive trees during drought stress: changes in activity of some antioxidant enzymes. Funct Plant Biol 32:45–53.
Sofo A, Dichio B, Montanaro G, Xiloyannis C (2009) Photosynthetic performance and light response of two olive cultivars under different water and light regimes. Photosynthetica 47:602–608.
Steudle E (2000) Water uptake by roots: effects of water deficit. J Exp Bot 51:1531–1542.
Steudle E (2001) The cohesion–tension mechanism and the acquisition of water by plant roots. Annu Rev Plant Physiol Plant Mol Biol 52:847–875.
Steudle E, Frensch J (1996) Water transport in plants: role of the apoplast. Plant Soil 187:67–79.
Steudle E, Peterson CA (1998) How does water get through roots? J Exp Bot 49:775–788.
Torres-Ruiz JM, Diaz-Espejo A, Chamorro V, Fernández JE, Sebastiani L, Minnocci A (2011) Influence of the water treatment on the xylem anatomy and functionality of current year shoots of olive trees. Acta Hortic 922:203–208.
Torres-Ruiz JM, Diaz-Espejo A, Perez-Martin A, Hernandez-Santana V (2015) Role of hydraulic and chemical signals in leaves, stems and roots in the stomatal behaviour of olive trees under water stress and recovery conditions. Tree Physiol 35:415–424.
Tyerman SD, Bohnert HJ, Maurel C, Steudle E, Smith JAC (1999) Plant aquaporins: their molecular biology, biophysics and significance for plant water relations. J Exp Bot 50:1055–1071.
Velikanov GA, Belova LP (2005) Regulation of water permeability of vacuolar symplast. Russ J Plant Physiol 52:758–764.
Willigen VC, Verdoucq L, Boursiac Y, Maurel C (2004) Aquaporins in plants. In: Blatt MR (ed.) Membrane transport in plants. Annual plant reviews 8. Blackwell Publishing, Sheffield, pp 221–250.
Xiloyannis C, Dichio B, Nuzzo V, Celano G (1999) Defense strategies of olive against water stress. Acta Hortic 474:423–426.
Ye Q, Steudle E (2006) Oxidative gating of water channels (aquaporins) in corn roots. Plant Cell Environ 29:459–470.